Acta Crystallographica Section B
Structural Science
ISSN 0108-7681

Cation movement and phase transitions in KTP isostructures; X-ray study of sodium-doped KTP at 10.5 K

Stefan T. Norberg,[a]* Alexander N. Sobolev[b] and Victor A. Streltsov[c]†

[a]Materials and Surface Chemistry, Chalmers University of Technology, SE-412 96 Göteborg, Sweden, [b]Chemistry Department, University of Western Australia, Nedlands, Western Australia 6907, Australia, and [c]Crystallography Centre, University of Western Australia, Nedlands, Western Australia 6907, Australia

† Present address: CSIRO HSN, 343 Royal Parade, Parkville, Victoria 3081, Australia

Correspondence e-mail: stn@inoc.chalmers.se

Received 22 January 2003
Accepted 14 April 2003

An accurate structure model of sodium-doped potassium titanyl phosphate, $(Na_{0.114}K_{0.886})K(TiO)_2(PO_4)_2$, has been determined at 10.5 K by single-crystal X-ray diffraction. In addition to the low-temperature data, X-ray intensities have been collected at room temperature. When the temperature was decreased from room temperature to 10.5 K, both potassium cations moved 0.033 (2) Å along the *c*-axis, *i.e.* in the polar direction within the rigid Ti—O—P network. This alkaline metal ion displacement can be related to the Abrahams–Jamieson–Kurtz T_C criteria for oxygen framework ferroelectrics. Potassium titanyl phosphate (KTP) is a well known material for second harmonic generation (SHG), and the influence of sodium dopant on the TiO_6 octahedral geometry and SHG is discussed. The material studied crystallizes in the space group $Pna2_1$ with $Z = 4$, $a = 12.7919\ (5)$, $b = 6.3798\ (4)$, $c = 10.5880\ (7)$ Å, $V = 864.08\ (9)$ Å^3, $T = 10.5\ (3)$ K and $R = 0.023$.

1. Introduction

The $KTiOPO_4$ (KTP, potassium titanyl phosphate) structure was determined by Tordjman *et al.* (1974) and has since evolved to a well known material for various non-linear optical applications. It is the material of choice in applications that utilize the second harmonic generation effect for laser-frequency doubling (Boulanger *et al.*, 1994), where a large second-order non-linear coefficient is needed. The thermal stability, chemical resistivity, high non-linearity and high optical damage threshold in combination with a wide optical transmission window are extended to many isostructural compounds. These compounds can be described with the general chemical formula $ATiOBO_4$ (most common are A = K, Rb, Cs or Tl and B = P or As; Stucky *et al.*, 1989, and references therein).

However, the number of KTP isostructures is immense. A complete list of them would include many compounds with reduced or almost non-existent non-linear optical coefficients. It is, for instance, possible to exchange titanium fully or partly during the growth of KTP isostructural crystals, *e.g.* $KSnOPO_4$ (Thomas *et al.*, 1990) and $KGe_{0.18}Ti_{0.82}OPO_4$ (Sorokina *et al.*, 1996). The most common atomic combinations that can form KTP-like structures are $AMOBO_4$ with A = K, Rb, Cs, Tl, Na, Ag or NH_3, M = Ti, Sn, Nb or Ge and B = P or As, but not all of these atomic combinations are easily crystallized as single crystals. Nevertheless, the overall multitude of compounds offers a great opportunity for the study of fundamental structurally related properties, such as pyroelectricity, ferroelectricity and non-linear optical susceptibility. In particular,

this is the case for properties related to the alkaline ion constituent in KTP structures. Sodium-doped KTP crystals grown by spontaneous flux methods are therefore good candidates for accurate structural studies.

Another reason for an extended structure and growth study of sodium-doped KTP crystals is a recent paper by Suma *et al.* (1998), which reports an alternative flux for the growth of KTP crystals, namely $KNaPO_3F$. Their result indicates the possibility to accomplish fast growth of large KTP crystals using spontaneous or seeded flux-growth techniques in combination with a very steep temperature ramp (5 K h^{-1}). The high growth rate is due to the low viscosity of the $KNaPO_3F$ flux compared with the $K_6P_4O_{13}$ flux (Jacco *et al.*, 1984), plus the slightly higher solubility of KTP in this new flux. A disadvantage is that sodium replaces a portion of the potassium in the KTP structure.

Two main methods have been used to produce sodium-doped KTP crystals. The first involves the immersion of small KTP crystals in molten $NaNO_3$ using platinum crucibles and elevated temperatures, typically 623 K, for a week or more. However, this technique produces opaque $Na_xK_{1-x}TiOPO_4$ crystals of poor quality owing to the harsh treatment of the crystals (Jarman, 1989; Phillips *et al.*, 1991). The second method is solid-state sintering (Voronkova *et al.*, 1990) that results in powders. There is, additionally, a third less explored method (Loiacono *et al.*, 1994), which involves replacing some of the potassium content by sodium in the flux used for the crystal growth. The later method cannot be used for complete exchange of potassium for sodium, as the maximum ratio of sodium and potassium that gives KTP isostructural crystals is $\sim$ 7:3.

The few sodium-doped KTP crystals that have been structurally characterized are either from solid-state sintering or sodium ion exchange, except for one case. The structure of $Na_{0.48}K_{0.52}TiOPO_4$ powder was determined by Crennell *et al.* (1991). Ion-exchanged crystals of $Na_{0.58}K_{0.42}TiOPO_4$ and $Na_{0.95}K_{0.05}TiOPO_4$ have been characterized by Crennell *et al.* (1992) and Phillips *et al.* (1992), respectively. Dahaoui *et al.* (1997, 1999) investigated the structure (at 100 K) and electrostatic properties (at temperatures between 100 and 600 K) of almost completely sodium-ion-exchanged KTP crystals, *i.e.* $Na_{0.99}K_{0.01}TiOPO_4$. Lee *et al.* (1997) determined the structure of a flux-grown $Na_{0.16}K_{0.84}TiOPO_4$ single crystal.

We have grown a series of sodium-doped KTP (NaKTP) crystals by the flux method. The crystal with the sodium-ion content described in this report is the first of them to be structurally characterized. This is also, to the best of our knowledge, the first low-temperature (*i.e.* below 70 K) measurement of a doped KTP crystal. The same single-crystal sample has also been structurally characterized at room temperature and it was discovered that both potassium cations are displaced along the polar *c*-axis in the rigid Ti—O—P network. We have demonstrated that this alkaline metal ion displacement could be related to the Abrahams–Jamieson–Kurtz (Abrahams, 1994) T_C criteria for ferroelectric oxygen framework structures. The cation coordination over a broad range of temperatures as well as the correlation between TiO_6 octahedra geometry distortions and the second harmonic generation strength are discussed.

2. Experimental

2.1. Crystallization

The crystal used in the X-ray diffraction experiment was grown by spontaneous crystallization from a flux, in a 35 ml platinum crucible, containing KH_2PO_4, NaH_2PO_4, K_2HPO_4, Na_2HPO_4 and TiO_2 carefully mixed together in the molar ratio 1.2:1.8:0.8:1.2:1. This mixture would correspond to the growth of $Na_xK_{1-x}TiOPO_4$ in a $Na_{3.6}K_{2.4}P_4O_{13}$ flux, *i.e.* a modified $K_6P_4O_{13}$ flux (Jacco *et al.*, 1984). The flux was slowly heated over 4 d up to 1273 K, kept at this temperature for 3 d in order to obtain a homogeneous melt and afterwards cooled to 1023 K by 1.4 K h^{-1}. The resulting crystals were easily recovered by dissolving the flux in water.

2.2. Data collection

The low-temperature (LT) data were collected on a locally assembled Huber 512 goniometer equipped with a Displex 202D cryogenic refrigerator similar to that reported by Larsen (1995). In order to improve counting statistics, the crystal studied was larger than normally used for single-crystal diffraction, as there was a significant absorption of the incident beam by the beryllium windows in the cryostat tube. Crystal faces were indexed using optical microscopy and the morphology was typical of that of KTP (Bolt & Bennema, 1990) with the dimensions given in Table 1. A full sphere of intensity profiles was collected in the ω–2θ scan mode up to $2\theta = 50^\circ$, extended as a half sphere up to $2\theta = 80^\circ$ and finally as a quarter sphere up to $2\theta = 100^\circ$. Corrections for absorption by the beryllium thermal shield were carried out with the *PROFIT* profile-fitting program (Streltsov & Zavodnik, 1989). The room-temperature (RT) data (full sphere measurement up to $2\theta = 50^\circ$) were collected ahead of the LT data in order to establish the presence of sodium dopant.

Both sets of collected X-ray intensities were corrected for experimental intensity variations, as indicated by standard reflections, and for absorption using an analytical model (Alcock, 1974). The analytical absorption correction reduced $R_{\rm int}(I)$ from 0.025 to 0.017 for the LT data and from 0.027 to 0.018 for the RT data. Symmetry-equivalent reflections were averaged while keeping Friedel mates separated. Further experimental details are given in Table 1.

2.3. Structure refinement

All X-ray intensities collected at 10.5 K were used in the structure refinement utilizing the *Xtal*3.71 software package (Hall *et al.*, 2000). The initial structural model did not include any sodium-dopant and was based on atomic parameters from Norberg *et al.* (2000). This refinement converged to $R = 0.023$, $wR = 0.047$, $S = 1.503$, with a residual electron density of $\Delta\rho_{\rm max}/\Delta\rho_{\rm min}$ of 4.88/−2.78 e Å^{-3} [$\sigma(\Delta\rho) = 0.06$ e Å^{-3}]. The residual electron density maps showed one significantly high peak in the vicinity of K1, with a K1 peak distance of

Table 1
Experimental table.

	10 K	RT
Crystal data		
Chemical formula	$(Na_{0.114}K_{0.886})K(TiO)_2(PO_4)_2$	$(Na_{0.114}K_{0.886})K(TiO)_2(PO_4)_2$
M_r	394.06	394.06
Cell setting, space group	Orthorhombic, $Pna2_1$	Orthorhombic, $Pna2_1$
a, b, c (Å)	12.7919 (5), 6.3798 (4), 10.588 (7)	12.806 (10), 6.3889 (6), 10.588 (10)
V (Å^3)	864.08 (9)	866.27 (13)
Z	4	4
D_x (Mg m^{-3})	3.029	3.021
Radiation type	Mo $K\alpha$	Mo $K\alpha$
No. of reflections for cell parameters	28	14
θ range (°)	19.5–38.3	19.5–23.7
μ (mm^{-1})	3.18	3.17
Temperature (K)	10.5 (3)	293 (2)
Crystal form, colour	Prism, colourless	Prism, colourless
Crystal size (mm)	0.30 × 0.30 × 0.21	0.30 × 0.30 × 0.21
Data collection		
Diffractometer	Huber 512 goniometer	Huber 512 goniometer
Data collection method	ω–2θ	ω–2θ
Absorption correction	Analytical	Analytical
T_{min}	0.389	0.428
T_{max}	0.521	0.513
No. of measured, independent and observed parameters	16 753, 8961, 8961	5704, 1539, 1539
Criterion for observed reflections	$F > 0\sigma(F)$	$F > 0\sigma(F)$
R_{int}	0.017	0.018
θ_{max} (°)	50.1	25.1
Range of h, k, l	$-15 \Rightarrow h \Rightarrow 27$ $-11 \Rightarrow k \Rightarrow 13$ $-22 \Rightarrow l \Rightarrow 22$	$-15 \Rightarrow h \Rightarrow 15$ $-7 \Rightarrow k \Rightarrow 7$ $-12 \Rightarrow l \Rightarrow 12$
No. and frequency of standard reflections	3 every 100 reflections	3 every 100 reflections
Intensity decay (%)	0.1	0.1
Refinement		
Refinement on	F	F
$R[F^2 > 2\sigma(F^2)]$, $wR(F^2)$, S	0.017, 0.037, 1.18	0.016, 0.024, 1.12
No. of reflections	8961	1539
No. of parameters	156	150
Weighting scheme	$w = 1/[\sigma^2(F) + 0.0015(F)^2]$	$w = 1/[\sigma^2(F) + 0.001(F)^2]$
$(\Delta/\sigma)_{max}$	0.001	<0.0001
$\Delta\rho_{max}$, $\Delta\rho_{min}$ (e Å^{-3})	1.67, −1.54	0.52, −0.34
Extinction method	Isotropic Gaussian (Zachariasen, 1967)	Isotropic Gaussian (Zachariasen, 1967)
Extinction coefficient	53×10^2 (2)	41×10^2 (3)
Absolute structure	Flack (1983) parameter refined	Flack (1983) parameter refined
Flack (1983) parameter	0.508 (13)	0.55 (3)

Computer programs: *PROFIT* (Streltsov & Zavodnik, 1989), *Xtal*3.71 (Hall *et al.*, 2000); programs: *DIFDAT*, *SORTRF*, *ADDREF*, *ABSORB*, *CRYLSQ*, *FOURR*, *SLANT*, *CONTRS*, *BONDLA*, *ATABLE*, *CIFIO*, *ORTEP*III for Windows (Farrugia, 1997).

0.569 (1) Å, see Fig. 1(*a*), and that position was described as the sodium dopant in subsequent refinements. The total occupancy of K1 and Na1 was constrained to 1 and all atomic positions were refined with anisotropic thermal displacement factors, which resulted in a $(Na_{0.114}K_{0.886})K(TiO)_2(PO_4)_2$ structure. The final $\Delta\rho$ maps, see Figs. 1(*b*)–(*d*), were without any significant peaks of positive residual electron density and indexes were $R = 0.017$, $wR = 0.037$, $S = 1.182$ and $\Delta\rho_{max}/\Delta\rho_{min}$ of 1.67/−1.54 e Å^{-3} [$\sigma(\Delta\rho) = 0.06$ e Å^{-3}].

An isotropic extinction parameter (Zachariasen, 1967) was refined for the LT structure using Larson's implementation (Larson, 1970). Almost 9% of the reflections were affected by extinction with a maximum correction of $y = 0.82$ for the 004 reflection (the observed structure factor is $F_{obs} = yF_{kin}$, where F_{kin} is the kinematic value). The refined Flack (1983) parameter of 0.508 (13) could indicate that the crystal used in the data collection contained an equal mixture of domains with opposite polarization, *i.e.* approximately 50% of the [001] inversion twin.

The RT structure was refined using the same atomic parameters as the LT structure, except that Na1 had an isotropic displacement parameter and was constrained to the same population parameter as determined for the LT structure [refinement with a non-constrained population parameter for Na1 resulted in an enlarged U_{eq} of 0.043 (10) Å^2 and a population parameter of 0.079 (7)]. The resulting RT structure had the following indexes: $R = 0.016$, $wR = 0.024$, $S = 1.123$ and $\Delta\rho_{max}/\Delta\rho_{min} = 0.52/-0.34$ e Å^{-3} [$\sigma(\Delta\rho) = 0.03$ e Å^{-3}]. About 27% of the reflections were affected by extinction with a maximum correction of $y = 0.84$ for the 022 reflection. The Flack parameter was refined to 0.55 (3).[1]

3. Result and discussion

3.1. Cation displacement

The archetypal structure of KTP has been well described in a number of earlier publications, see for example Stucky *et al.* (1989) or Thomas *et al.* (1990). The isostructural NaKTP has the characteristically deformed TiO_6 octahedra with unusual short/long Ti—O bonds, and loosely bounded alkaline cations in

[1] Supplementary data, including occupation and displacement parameters for NaKTP at 10.5 K and RT, for this paper are available from the IUCr electronic archives (Reference: OS0106). Services for accessing these data are described at the back of the journal.

structural cages that result in a highly anisotropic ionic conductivity. All relevant bond distances at RT and 10.5 K are given in Table 2. The NaKTP structures at RT and 10.5 K are depicted as thermal ellipsoid plots in Fig. 2.

No phase transition was detected between RT and 10.5 K, and the rigid network of TiO_6 octahedra and PO_4 tetrahedra showed only insignificant shifts of atomic positions. Changes in the Ti—O and P—O bond distances were primarily due to unit-cell contraction with temperature drop, and the only detectable movements of atomic positions were those of the alkaline cations. Both K1 and K2 moved 0.033 (2) Å along the polar direction of the ferroelectric KTP structure. These potassium cation movements are in good agreement with those measured for the rubidium cations in the $RbTiOAsO_4$ structure (Almgren *et al.*, 1999). There it was found that both Rb1 and Rb2 moved ~0.04 (1) Å along the polar axis between 295 and 9.6 K.

Our study of KTP with a small amount of sodium dopant at 10.5 and 293 K can complement the high-temperature investigation of KTP by Delarue *et al.* (1999). They collected accurate single-crystal X-ray diffraction data for KTP at 293, 673 and 973 K in order to observe the behaviour of the potassium cations at elevated temperatures. It was found that both potassium sites were separated into multiple sites spread in the *c*-axis direction at temperatures between 293 and 673 K. The initial potassium sites and their corresponding satellite sites were further separated, and the initially low occupancy parameters of the satellite sites increased slowly with temperature. It is sensible to propose that this separation of the alkaline-split positions and equalization of the occupancy is likely to continue until the structure reaches T_C and transforms from the ferroelectric to the paraelectric phase, *i.e.* from space group $Pna2_1$ to *Pnan*. Fig. 3 combines our data with those of Delarue *et al.* (1999). It indicates a likely evolution of the alkaline-split positions between 973 K and the T_C of 1207 K (Stefanovich *et al.*, 1996), as no KTP single-crystal X-ray diffraction has been carried out at temperatures above 973 K. This model of structural phase transition with split positions above and below the phase transition point has been established for some KTP-like structures with a low T_C, such as ASbO[Ge,Si]O_4 compounds with T_C below 500 K (see, for example, Belokoneva *et al.*, 1997). It would also be reasonable to expect similar alkaline-split positions at room temperature for ATiOBO$_4$ (A = K, Rb, Cs or Tl and B = P or As) compounds with a T_C well below that of KTP. One such compound is $CsTiOAsO_4$ with a T_C of 943 K (Marnier *et al.*,

Table 2
Selected geometric parameters (Å) for NaKTP.

	10.5 K	293 K
K1—O1	2.8601 (10)	2.887 (3)
K1—O2	2.7365 (9)	2.727 (3)
K1—O3^{i}	2.7034 (9)	2.702 (2)
K1—O11	2.9513 (9)	2.998 (3)
K1—O12^{i}	2.7048 (9)	2.715 (3)
K1—O5^{ii}	2.8437 (10)	2.877 (4)
K1—O7^{ii}	3.0229 (9)	3.061 (3)
K1—O8	2.741 (2)	2.755 (8)
Na1—O1	2.896 (6)	2.98 (2)
Na1—O3^{i}	2.833 (5)	2.78 (2)
Na1—O11	2.563 (6)	2.71 (2)
Na1—O12^{i}	2.582 (6)	2.53 (2)
Na1—O5^{ii}	2.613 (6)	2.73 (2)
Na1—O7^{ii}	2.665 (6)	2.75 (2)
Na1—O8	2.594 (7)	2.60 (2)
K2—O1^{iii}	2.6854 (9)	2.685 (3)
K2—O2^{ii}	2.9412 (9)	2.974 (3)
K2—O3^{ii}	3.0027 (11)	3.030 (3)
K2—O4^{iv}	3.1348 (9)	3.108 (2)
K2—O11	2.7635 (9)	2.760 (3)
K2—O12^{ii}	3.0348 (9)	3.057 (3)
K2—O5^{v}	2.7940 (8)	2.798 (2)
K2—O7^{ii}	2.9078 (9)	2.922 (3)
K2—O8^{ii}	3.017 (4)	3.042 (14)
Ti1—O1	2.1469 (10)	2.150 (3)
Ti1—O2^{vi}	1.9619 (9)	1.957 (3)
Ti1—O11	1.9800 (9)	1.981 (3)
Ti1—O12^{ii}	1.7253 (9)	1.719 (3)
Ti1—O5^{ii}	2.0356 (8)	2.045 (2)
Ti1—O6^{vii}	1.9769 (8)	1.985 (2)
Ti2—O3	2.0393 (8)	2.043 (2)
Ti2—O4^{v}	1.9730 (8)	1.978 (2)
Ti2—O11	1.7444 (9)	1.739 (3)
Ti2—O12	2.0872 (9)	2.091 (3)
Ti2—O7^{vii}	1.9723 (10)	1.969 (3)
Ti2—O8	1.992 (5)	1.988 (18)

Symmetry codes: (i) $x, y-1, z$; (ii) $\frac{1}{2}-x, y-\frac{1}{2}, z-\frac{1}{2}$; (iii) $x-\frac{1}{2}, \frac{1}{2}-y, z$; (iv) $x-\frac{1}{2}, \frac{3}{2}-y, z$; (v) $-x, 1-y, z-\frac{1}{2}$; (vi) $1-x, 1-y, z-\frac{1}{2}$; (vii) $\frac{1}{2}-x, \frac{1}{2}+y, z-\frac{1}{2}$.

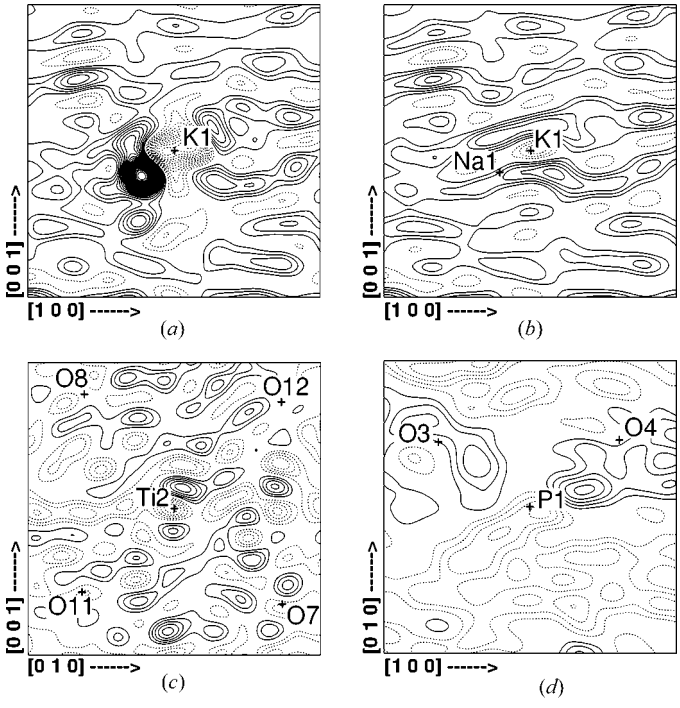

Figure 1
$\Delta\rho$ maps for sodium-doped KTP with positive and negative contours as solid lines and dashed lines, respectively, at increments of 0.2 e Å^{-3} [$\sigma(\Delta\rho)$ = 0.06 e Å^{-3}]. The zero contours are omitted. The maps show $\Delta\rho$ (*a*) before and (*b*) after the addition of a sodium site close to the K1 position; (*c*) in the Ti2 octahedra and (*d*) the P1 tetrahedra after the structure refinement. All O atoms in (*c*) and (*d*) are located in the close vicinity of the depicted plane. Map borders are 4 × 4 Å.

1989), in which Nordborg (2000) detected previously undiscovered caesium-split positions at room temperature.

We have used the fractional atomic coordinates determined by Delarue *et al.* (1999) in order to calculate the shift for the initial potassium positions between 293 and 973 K; K1 moved 0.061 (2) Å and K2 moved 0.082 (2) Å along the *c*-axis. These distances are in good agreement with our measured displacements between 10.5 and 293 K, and give a total cation movement of 0.11 (1) Å between 10.5 and 973 K. No single-crystal structure data for KTP at temperatures above 973 K are available, but it would be reasonable to suggest that the cation displacement between 973 and T_C is probably as large as the displacement between 10.5 and 973 K, or slightly higher as the rate of cation displacement along the *c*-axis might increase with an increase in temperature.

The Abrahams–Jamieson–Kurtz oxygen-framework T_C criteria (Abrahams, 1994)

$$T_C = (K/2k)(\Delta z)^2 \text{ K},$$

where K is a force constant, k is Boltzmann's constant, Δz is the largest displacement component along the polar direction from the zero spontaneous polarization position, with $(K/2k)$ approximated to 2.00 (9) $\times 10^4$ K Å^{-2}, has not been successfully used for ferroelectric ATiOBO$_4$-type structures (A = K, Rb, Cs or Tl and B = P or As). The KTP's T_C of 1207 K gives a Δz displacement of 0.24 (1) Å, which is a likely displacement along the *c*-axis for the initial cation sites. This would indicate that the Abrahams–Jamieson–Kurtz T_C criteria could be used to approximate the phase transition temperature of the KTP isostructural compounds. It might just be a matter of selecting an appropriate cation position that shows pure displacement in the rigid Ti—O—P network, *i.e.* a cation position that is occupied before position splitting rather than one that appears at elevated temperatures only. This is of course problematic for compounds with low T_C as they could have alkaline-split positions down to liquid helium temperatures.

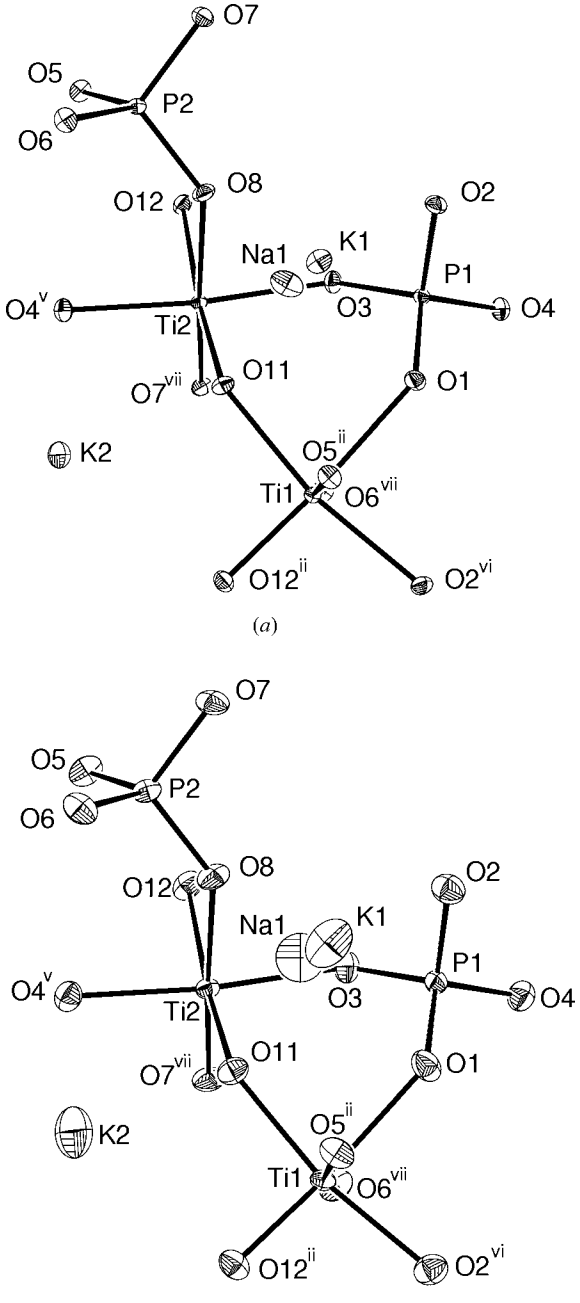

Figure 2
Thermal ellipsoid plots of the NaKTP structure at (*a*) low and (*b*) ambient temperatures as projected on the (010) plane. Displacement ellipsoids are drawn at the 80% probability level. Symmetry codes are given in Table 2.

3.2. Cation coordination

The small amount of sodium dopant has almost negligible effect on the unit-cell dimensions and all sodium cations are situated in the smaller of the two possible cation cages (K1). This is the preferred sodium location in all sodium-doped KTP structures determined (see §1 for references). The corresponding cation–oxygen interatomic distances confirm the location of K1 and Na1 in two separate atomic positions. K1 is coordinated by eight O atoms with bonding distances in the interval 2.7034 (9)–3.0229 (9) Å. This gives the mean bond

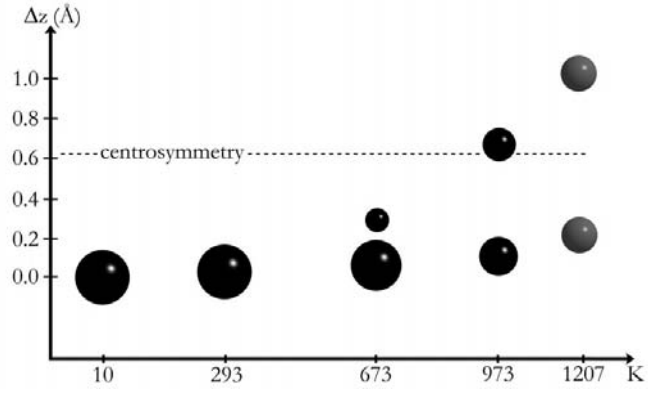

Figure 3
Potassium displacement in KTP: relative Δz (Å) movement is plotted *versus* the crystalline temperature (K). The atomic sizes represent the occupancy parameter at each respective site. Grey atoms at 1207 K show the likely atomic positions for potassium at the ferroelectric to paraelectric phase transition.

Table 3
Evolution of the K2—O (Å) environment over the temperature range 105–973 K.

10.5 K: as determined in this report; 293 K: atomic coordinates from Delarue *et al.* (1999) are used, ours coincide extremely well with theirs but have slightly higher standard uncertainty; 673 and 973 K: Delarue *et al.* (1999).

	10.5 K	293 K	673 K	973 K
a (Å)	12.7919 (5)	12.807 (1)	12.844 (1)	12.907 (2)
b (Å)	6.3798 (4)	6.3981 (5)	6.4245 (7)	6.4609 (8)
c (Å)	10.5880 (7)	10.583 (1)	10.579 (1)	10.559 (2)
K2—O1	2.685 (1)	2.680 (1)	2.659 (1)	2.704 (2)
K2—O2	2.941 (1)	2.974 (1)	2.974 (1)	3.114 (2)
K2—O3	3.003 (1)	3.035 (1)	3.037 (1)	3.113 (2)
K2—O4	3.135 (1)	3.121 (1)	3.170 (1)	3.086 (2)
K2—O11	2.763 (1)	2.760 (1)	2.794 (1)	2.771 (2)
K2—O12	3.035 (1)	3.050 (1)	3.068 (1)	3.118 (2)
K2—O5	2.794 (1)	2.803 (1)	2.827 (1)	2.839 (2)
K2—O7	2.908 (1)	2.910 (1)	2.882 (1)	2.939 (2)
K2—O8	3.017 (4)	3.038 (1)	3.010 (1)	3.113 (2)
Mean K2—O†	2.92 (14)	2.93 (15)	2.97 (16)	2.98 (17)
BVS‡	1.15	1.13	1.11	1.01

† Standard uncertainty calculated as: $\left[\sum(x-\bar{x})^2/(n-1)^{1/2}\right]$. ‡ From bond-valance calculations (Brown & Altermatt, 1985).

distance of 2.82 (12) Å. On the other hand, Na1 is coordinated by seven O atoms at 2.563 (6)–2.896 (6) Å from the sodium site and has the mean bond distance of 2.68 (13) Å. The coordination polyhedra of the sodium and potassium sites are depicted in Fig. 4. K2 from the larger cation cage is coordinated by nine O atoms with bonding distances ranging from 2.6854 (9) to 3.1348 (9) Å and the mean bond length of 2.92 (14) Å. The bond-length analysis clearly shows that it is the sodium position that has been refined as Na1, and in accordance with the high-temperature study by Delarue *et al.* (1999) indicating that the potassium split positions in KTP appear well above RT.

The Ti—O—P network rigidity forces the incorporated sodium to occupy a new cation site, which is positioned closer to O11 than the corresponding potassium site. This gives a short bond distance between the sodium dopant and the O11 titanyl oxygen atom, and in turn more appropriate Na—O bond distances. However, it should be noted that both the K1 and K2 cation cages are too large for the small sodium cation, which has an ionic radius of 1.12 Å compared with 1.51 Å for potassium (Shannon, 1976). The great difference in ionic radii and ability to fit in the cation cages is for example exemplified by the fact that $NaTiOPO_4$ cannot be flux grown as a KTP isostructure, since the cations are too small to stabilize the Ti—O—P network during crystallization. Instead a centrosymmetric monoclinic structure related to $CaTiOSiO_4$ (titanite) crystallizes (Phillips *et al.*, 1992).

The cation coordination environment alters with temperature and those changes for the K2 atomic site are given in Table 3, which also tabulates bond-valance sum (BVS) calculations (Brown & Altermatt, 1985) for the K2 site. The BVS calculations and the continuous increase of the mean K2—O bond distance show that K2 moves toward the less constrained atomic site at higher temperatures. This effect is related to the changes in unit-cell dimensions, cation position displacement and increased thermal displacement parameters, with the temperature rise. K2 vibrates predominantly in the [001] direction, while K1 vibrates predominantly in the [101] direction.

3.3. Electron density

The electron density analysis in the KTP structure has been carried out by Hansen *et al.* (1991) at room temperature and by Larsen (1995) at 9 K. They observed an excess of the difference electron density in the Ti—O bonds related to a strong covalent bonding. This led to the suggestion that the non-linear optical properties could be explained by hyperpo-

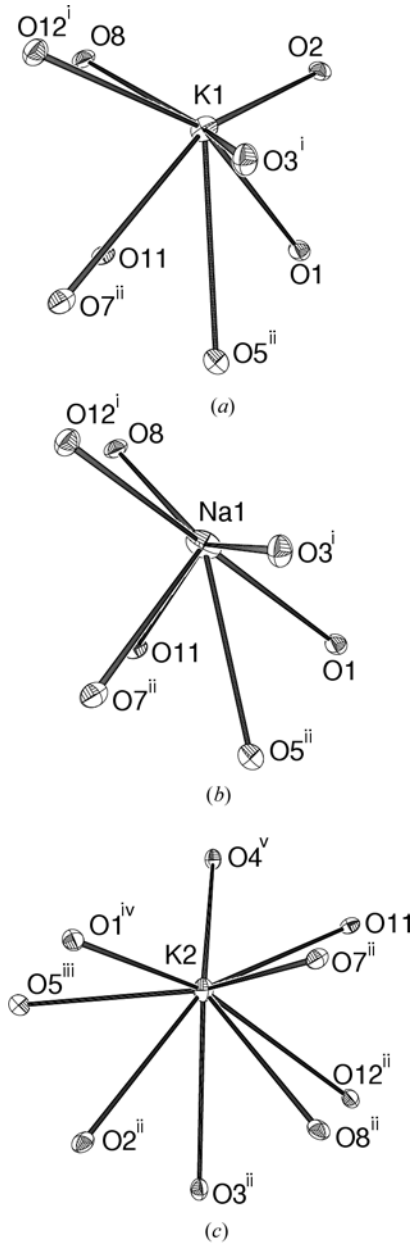

Figure 4
Views of the (*a*) K1, (*b*) Na1 and (*c*) K2 cation–oxygen coordination in NaKTP. Displacement ellipsoids are as in Fig. 2 and symmetry codes as in Table 2.

Table 4
Geometric changes (Å) to the TiO_6 octahedra for $Na_xK_{1-x}TiOPO_4$ compounds with increasing x.

	$KTiOPO_4$	$Na_{0.06}K_{0.94}TiOPO_4$	$Na_{0.16}K_{0.84}TiOPO_4$	$Na_{0.57}K_{0.43}TiOPO_4$	$Na_{0.95}K_{0.05}TiOPO_4$	$Na_{0.99}K_{0.01}TiOPO_4$
$(Ti1-O)_{max}$	2.150 (2)	2.147 (1)	2.155 (2)	2.157 (1)	2.226	2.229 (1)
$(Ti1-O)_{min}$	1.716 (2)	1.725 (1)	1.715 (1)	1.728 (1)	1.717	1.710 (1)
$\Delta(Ti1-O)$	0.43	0.42	0.44	0.43	0.51	0.52
$(Ti2-O)_{max}$	2.092 (4)	2.087 (1)	2.096 (2)	2.097 (1)	2.099	2.093 (1)
$(Ti2-O)_{min}$	1.733 (3)	1.744 (1)	1.735 (2)	1.741 (1)	1.758	1.756 (1)
$\Delta(Ti2-O)$	0.36	0.34	0.36	0.36	0.34	0.34
SHG†	Good	Good	Good	Not bad	Poor	Poor

† As determined by Phillips *et al.* (1992): not bad represents slightly decreased SHG compared with KTP, while poor is below one-tenth of KTP's SHG.

larization of Ti—O bonds. Satellite peaks close to the potassium ions were also observed, which were greatly reduced by refining diffuse non-spherical multipole functions at the potassium sites. However, the best modelling of the experimental data for the isostructural $RbTiOAsO_4$ (RTA) by Streltsov *et al.* (2000) was obtained with the Rb atoms in split positions. The strong accumulation of the difference charge density near the Rb atoms at a distance of ~ 0.5 Å along the *c*-axis was attributed to the partial occupancy of additional sites. Rubidium-split positions are well pronounced in RTA at room temperature, since RTA has a T_C significantly lower than that of KTP, *i.e.* 1073 K (Marnier *et al.*, 1989). This type of temperature-dependent disorder is evidently common for the KTP family of compounds (Belokoneva *et al.*, 1997; Delarue *et al.*, 1999) and could be expected to some degree in KTP itself.

The difference density features in Figs. 1(*b*)–(*d*) are similar to those obtained in KTP and RTA using conventional independent atom model (IAM) refinement. The observed features such as peaks near the Ti atoms showing a dipole-like density oriented parallel to the *c*-axis. However, those features changed in a similar way in both KTP (Hansen *et al.*, 1991) and RTA (Streltsov *et al.*, 2000) when the difference density maps were calculated using phases from the multipole refinement, emphasizing the importance of thorough non-spherical density models for non-centrosymmetric structures when it comes to the electron density evaluation. Such multipole refinement has not been attempted in the present study.

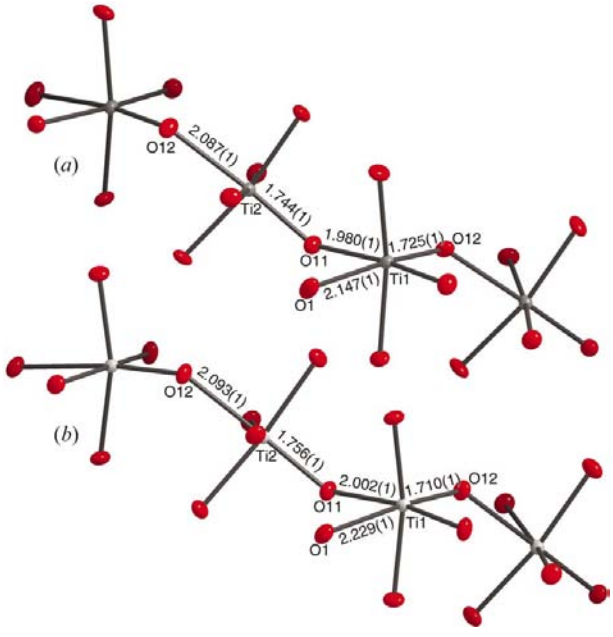

Figure 5
Views of the Ti—O—Ti chains in (*a*) the present study and (*b*) $Na_{0.99}K_{0.01}TiOPO_4$.

3.4. TiO_6 octahedral geometry and SHG

The second harmonic generation (SHG) intensity of $Na_xK_{1-x}TiOPO_4$ powder samples has been determined to be approximately constant up to $x = 0.55$ (Phillips *et al.*, 1995). Higher sodium concentrations result in a loss of SHG intensity compared with pure KTP and this decrease of SHG can be related to changes in the alkaline metal and TiO_6 coordination polyhedra. Both crystallographically independent TiO_6 octahedra have a short Ti—O titanyl bond (Ti1—O12 and Ti2—O11) and share their O11 and O12 vertices to form chains of alternating Ti1 and Ti2 octahedra. On the other hand, Ti2—O12 is the longest and Ti1—O11 is one of the longest bonds in the TiO_6 octahedra (see Table 2). Additionally, both O11 and O12 are involved in alkaline cation coordination sphere. The K1—O12 bond of 2.7048 (9) Å is almost the shortest, while the K1—O11 bond of 2.9513 (9) Å is one of the longest bonds in the K1—O coordination. However, the Na1—O11 bond distance of 2.563 (6) Å is the shortest in the Na1—O coordination polyhedron and the Na1—O12 bond distance of 2.582 (6) Å is close to that.

Geometric changes in the TiO_6 groups owing to sodium dopant have been tabulated in Table 4. All accurate single-crystal studies of sodium-doped KTP (present work and those cited in §1) have been included together with KTP data (Thomas *et al.*, 1990). Increased sodium content results in shorter Ti1—O12 bonds and longer Ti1—O11 bonds, while there is no evident change in the distortion of the Ti2 octahedra. Fig. 5 illustrates the Ti—O—Ti chain of $Na_{0.06}K_{0.94}TiOPO_4$ (NaKTP) and $Na_{0.99}K_{0.01}TiOPO_4$ (NaTP; Dahaoui *et al.*, 1997). The O atoms connecting TiO_6 octahedra occupy *cis*-positions in Ti1 and *trans*-positions in Ti2. It is

evident from Fig. 5 that the Ti1 octahedron is more distorted in the fully sodium substituted KTP.

The higher distortion of the Ti1 octahedron is also related to significant changes in the K2/Na2—O1 distances. The Na2—O1 bond distance in NaTP is 2.365 (1) Å (Dahaoui *et al.*, 1997), compared with the K2—O1 bond distance of 2.6854 (9) Å in NaKTP. This leads to increased Ti1—O1 bond distances in NaTP compared with NaKTP (see Fig. 5 and Table 4). The Ti1—O1 bond distance is 2.1469 (10) Å in NaKTP and 2.229 (1) Å in NaTP (Dahaoui *et al.*, 1997).

Thus, the interaction between the sodium cation and the bridging O atoms of the Ti—O—Ti chains is stronger than the corresponding interaction for the potassium cation. These interactions result in an increased distortion of the Ti1 octahedra for NaTP. The greater distortion leads to larger differences of short and long bond distances between the $Ti1O_6$ and $Ti2O_6$ groups. That seems to preclude a required charge transfer along the Ti—O—Ti chains, which is favourable for the non-linear optical property.

There is a need for more single-crystal studies of sodium-doped KTP in the dopant range 60–90% sodium inclusion in order to clarify the structural mechanism that decreases the non-linear optical susceptibility. It would also be sensible to examine the cation displacement for other KTP isostructures with large non-linear optical effect. This should be done over a wide temperature range, *i.e.* from 10 K to T_C, and for example $CsTiOAsO_4$ could be a suitable candidate as it has a relatively low T_C and alkaline-split positions at room temperature.

SN would like to thank the Crystallography Centre, UWA, for hospitality during the X-ray measurements for this work. Financial support from the Swedish Research Council is gratefully acknowledged. The authors are indebted to Professor Jörgen Albertsson and Dr Göran Svensson for helpful discussions, and to Professor Brian N. Figgis for use of the diffractometer.

References

Abrahams, S. C. (1994). *Acta Cryst.* A**50**, 658–685.
Alcock, N. W. (1974). *Acta Cryst.* A**30**, 332–335.
Almgren, J., Streltsov, V. A., Sobolev, A. N., Figgis, B. N. & Albertsson, J. (1999). *Acta Cryst.* B**55**, 712–720.
Belokoneva, E. L., Knight, K. S., Davids, W. I. F. & Mill, B. V. (1997). *J. Phys. Condens. Matter*, **9**, 3833–3851.
Bolt, R. J. & Bennema, P. (1990). *J. Cryst. Growth*, **102**, 329–340.
Boulanger, B., Feve, J. P., Marnier, G., Menaert, B., Cabirol, X., Villeval, P. & Bonnin, C. (1994). *J. Opt. Soc. Am. B*, **11**, 750–757.
Brown, I. D. & Altermatt, D. (1985). *Acta Cryst.* B**41**, 244–247.
Crennell, S. J., Morris, R. E., Cheetham, A. K. & Jarman, R. H. (1992). *Chem. Mater.* **4**, 82–88.
Crennell, S. J., Owen, J. J., Grey, C. P., Cheetham, A. K., Kaduk, J. A. & Jarman, R. H. (1991). *J. Mater. Chem.* **1**, 113–119.
Dahaoui, S., Hansen, N. K. & Menaert, B. (1997). *Acta Cryst.* C**53**, 1173–1176.
Dahaoui, S., Hansen, N. K., Protas, J., Krane, H.-G., Fischer, K. & Marnier, G. (1999). *J. Appl. Cryst.* **32**, 1–10.
Delarue, P., Lecomte, C., Jannin, M., Marnier, G. & Menaert, B. (1999). *J. Phys. Condens. Matter*, **11**, 4123–4134.
Farrugia, L. J. (1997). *J. Appl. Cryst.* **30**, 565.
Flack, H. D. (1983). *Acta Cryst.* A**39**, 876–881.
Hall, S. R., du Boulay, D. J. & Olthof-Hazekamp, R. (2000). Editors. *Xtal*3.71. University of Western Australia, Australia.
Hansen, N. K., Protas, J. & Marnier, G. (1991). *Acta Cryst.* B**47**, 660–672.
Jacco, J. C., Loiacono, G. M., Jaso, M., Mizell, G. & Greenberg, B. (1984). *J. Cryst. Growth*, **70**, 484–488.
Jarman, R. H. (1989). *Solid State Ion.* **32**/**33**, 45–49.
Larsen, F. K. (1995). *Acta Cryst.* B**51**, 468–482.
Larson, A. C. (1970). *Crystallographic Computing*, edited by F. R. Ahmed, S. R. Hall & C. P. Huber, pp. 291–294. Copenhagen: Munksgaard.
Lee, D. Y., Sorokina, N. I., Voronkova, V. I., Yanovskii, V. K., Verin, I. A. & Simonov, V. I. (1997). *Crystallogr. Rep.* **42**, 218–225.
Loiacono, G. M., Loiacono, D. N. & Stolzenberger, R. A. (1994). *J. Cryst. Growth*, **144**, 223–228.
Marnier, G., Boulanger, B. & Menaert, B. (1989). *J. Phys. Condens. Matter*, **1**, 5509–5513.
Norberg, S. T., Streltsov, V. A., Svensson, G. & Albertsson, J. (2000). *Acta Cryst.* B**56**, 980–987.
Nordborg, J. (2000). *Acta Cryst.* C**56**, 518–520.
Phillips, M. L. F., Harrison, W. T. A. & Stucky, G. D. (1991). *SPIE Int. Soc. Opt. Eng.* **1561**, 84–92.
Phillips, M. L. F., Harrison, W. T. A. & Stucky, G. D. (1995). *Appl. Phys. Lett.* **66**, 3069–3070.
Phillips, M. L. F., Harrison, W. T. A., Stucky, G. D., McCarron, E. M., Calabrese, J. C. & Gier, T. E. (1992). *Chem. Mater.* **4**, 222–233.
Shannon, R. D. (1976). *Acta Cryst.* A**32**, 751–767.
Sorokina, N. I., Voronkova, V. I., Yanovskii, V. K., Verin, I. A. & Simonov, V. I. (1996). *Crystallogr. Rep.* **41**, 432–435.
Stefanovich, S., Mosunov, A., Mill, B. & Belokoneva, E. (1996). *Ferroelectrics*, **185**, 63–66.
Streltsov, V. A., Nordborg, J. & Albertsson, J. (2000). *Acta Cryst.* B**56**, 785–792.
Streltsov, V. A. & Zavodnik, V. E. (1989). *Sov. Phys. Crystallogr.* **34**, 824–828.
Stucky, G. D., Phillips, M. L. F. & Gier, T. E. (1989). *Chem. Mater.* **1**, 492–509.
Suma, S., Santha, N. & Sebastian, M. T. (1998). *Mater. Lett.* **34**, 322–325.
Thomas, P. A., Glazer, A. M. & Watts, B. E. (1990). *Acta Cryst.* B**46**, 333–343.
Tordjman, I., Masse, R. & Guitel, J. C. (1974). *Z. Kristallogr.* **139**, 103–115.
Voronkova, V. I., Shubentsova, E. S. & Yanovskii, V. K. (1990). *Inorg. Mater.* **26**, 115–118.
Zachariasen, W. H. (1967). *Acta Cryst.* **23**, 558–564.